Elastic Scattering, Production Process and Their Relation in High Energy Nucleon-Nucleon Collisions

Masaru DOI

Department of Physics, Osaka University

Toyonaka, Osaka, 560, Japan

Elastic Scattering, Production Process and Their Relation in High Energy Nucleon-Nucleon Collisions

Masaru DOI
Department of Physics, Osaka University
Toyonaka, Osaka, 560, Japan

Abstract

The production process, $N+N \rightarrow N+N+n\pi$, is investigated on the basis of the covariant field theory. Production amplitude as well as elastic one is calculated under the special assumption about production mechanism. The eikonal approximation for nucleon trajectories is introduced, so these amplitudes are expressed in an impact parameter representation. They satisfy the s-channel unitarity for the elastic process.

The Feynman scaling behavior for the pion inclusive spectra is reduced as an automatic consequence of the present model. Furthermore, the difference between the transverse and longitudinal distribution of pion momenta can be explained. The imaginary part of the phase shift in an elastic channel is reduced as a reflection of the production process, and it reproduces diffractive properties for the elastic differential cross section.

Comparisons with p-p scattering data are made for various physical observables, namely, inclusive spectra for pions, average multiplicity, elastic and production cross sections,and elastic differential cross section. Agreements are fairly satisfactory.

§1 Introduction

Experimental data on high energy elastic scattering of hadrons exhibit diffractive properties. For example, there is a steep forward peak, and the elastic scattering amplitude is predominantly imaginary. Furthermore, the energy dependence of the total cross section is nearly constant, or at most $(\ln s)^2$ as shown by recent I.S.R. data[1], where s is center of mass energy squared. These features are reflected in phase shifts, which are demanded to be mainly imaginary and to have a weak energy dependence.

As a consequence of unitarity, the imaginary part of the phase shift should be interpreted as the absorption of the incident wave into many open inelastic channels. In the range of energy which we shall consider, particle production is the main part of inelastic processes. And so, the production mechanism should be taken into consideration in order to interpret the diffractive features.

On the other hand, as characteristic features of produced particles, it is observed experimentally that their transverse momenta $k_\perp$ are very small in comparison with longitudinal momenta $k_{//}$. In addition, Feynman[2] has conjectured that the so-called inclusive spectra of produced particles show a scaling behavior at sufficiently high energies;

$$k_0 \frac{d\sigma}{d^3k} = F(k_\perp, k_{//}, s) \underset{s\to\infty}{\simeq} f(k_\perp, x), \qquad (1.1)$$

where

$$x = k_{//}/k_{max} \simeq \frac{2}{\sqrt{s}} k_{//} , \qquad (1.2)$$

and k_0 stands for the energy of the produced particle. Experiments seem to support this conjecture fairly well.

The aim of this article is to investigate whether or not these experimental features can be reproduced consistently for both elastic scattering and production processes.

First, it is necessary to derive the relation between elastic scattering and production processes. This problem has been investigated by Calucci, Jengo and Rebbi[3], by Aviv, Sugar and Blankenbecler[4], and by Freid[5]. In the present article, the production amplitude as well as elastic one will be calculated on the basis of covariant field theory by assuming a production mechanism. Especially, it will be discussed in detail how the imaginary part of the phase shift in the elastic channel is related to our production mechanism.

The inclusive spectra for emitted pions will be expressed by our production amplitude. Then, it will be investigated whether or not we can reduce the Feynman scaling behavior and explain the characteristic difference between $k_\perp$ and $k_{//}$ spectra.

Finally, we would like to examine to what extent our field theoretical calculations based on the production mechanism can explain consistently various experimentally observed quantities; namely, the inclusive spectra $k_0 d\sigma/d\vec{k}$, the average pion multiplicity $\langle n \rangle$, the cross section for n pion production σ_n, the elastic differential cross section $d\sigma/dt$, and the total cross section σ_T.

The production model in this paper is as follows. High energy incident nucleons go almost straightforward, and interact each other by the so-called chain, which is assumed to be vector meson in this paper. Here a postulate is introduced that pion fields $\varphi(x)$ couple only with vector mesons, not directly with the nucleons. Then, possible diagrams for the pion production from one chain are shown in Fig.1. Let us consider, however, a production mechanism such that a number of pions are emitted as a consequence of a superposition of only the first diagram, Fig.1(a); that is, our production diagrams are s-channel crossed ladders, as shown in Fig.2. Thus, the pion fields $\varphi(x)$ are either emitted as external particles, or contracted each other as virtual particles connecting two chains. Our model for the production mechanism does not include diagrams corresponding to the emission of more than one pion from one chain, Fig.1(b) and so on. Therefore, our model is different from multi-peripheral models[6], in which all produced pions are emitted from one chain.

The selection of the production mechanism that only one pion is emitted from one chain is due to the following reasons. This produced pion is connected directly with each of nucleons through one virtual vector meson. While, the meson cloud around the nucleon is deformed by the Lorentz factor, γ, and this deformation is maintained during the high energy scattering process, because both nucleons are not deflected strongly. Therefore, momenta of our pions receive the direct influences from both nucleon clouds. Thus, it is expected that the transverse momentum $k_\perp$ of our pion

is small in comparison with its longitudinal momentum $k_{//}$ and that the relation between them is roughly $k_{\perp} \simeq k_{//}/\gamma$. These circumstances will be mathematically expressed in §3. On the other hand, in the case where two or more pions are emitted from one chain, the strong limitation due to the nucleon clouds on the pion momentum cannot be expected, because there exist vector mesons which do not interact directly with nucleons in the field theoretical point of view.

Next, we shall consider the type of interaction among nucleon, vector meson and pion. The simplest model is that two different vector mesons (V_{μ}'s) couple with one pion (φ), as shown in Fig.3(a). Since the interaction Lagrangian for this (V-V'-φ) coupling includes the derivative about the pion field. The S-matrix element based on this model is proportional to the pion momentum, strictly speaking, square of transverse momentum, $k_{\perp}^2$. This disagrees with the experimental fact. We shall not consider this model, although we can not yet definitely conclude whether or not the contribution from this model can be small for the non-zero coupling constant of the (V-V'-φ) vertex.

As the second realistic model which includes no derivative of the pion field, it is interested to consider the type of vertex among vector meson (V_{μ}), psedovector meson (A_{μ}), and psedoscalar meson (φ), as shown in Fig.3(b).

Since spin effect is not important at sufficiently high energy, it is convenient to treat the nucleon as a scalar particle. Then, as another simple model, scalar nucleon couples with vector mesons,

and then scalar meson is emitted from these vector mesons, as shown in Fig.3(c). It is clear from the characters of these vertices that the second (Fig.3(b)) and the third (Fig.3(c)) model give effectively the same momentum and energy dependence of the S-matrix element in the sufficiently high energy regions. Therefore, in this paper we shall investigate various features of the physical observables by using the third model. Hereafter, the scalar meson will be called as pion, and all vector mesons will be simply treated as the same.

In §2, calculations of the S-matrix elements corresponding to diagram in Fig.2 are performed with the aid of functional derivative methods[7] and by introducing an eikonal approximation about the nucleon[8]. It is shown that not only production amplitudes but also elastic one can be expressed in an impact parameter representation. The imaginary part of the phase shift in an elastic channel is derived, and its relation to the production processes is stated. In §3 is shown the appearance of the Lorentz factor, representing the Lorentz contraction of the meson clouds. Some of physical observables are expressed in terms of the phase shift. Furthermore, it is proved that our amplitudes satisfy the s-channel unitarity relation for the elasric process. In §4 is shown realization of the Feynman scaling behavior, which plays an essential role in our model in order to explain the difference between $k_{\perp}$ and $k_{//}$ spectra. Our numerical results for physical observables are compared with proton-proton collision data; especially relations between elastic and production channels are investigated. Conclusions and discussions apear in §5.

§2 Model calculation

Production amplitudes together with elastic one are determined on the basis of the special production mechanism and of the covariant field theory. We shall consider the case where two fast incident particles, nucleons, collide and eventually emit arbitrary number of pions. In order to obtain a closed form for scattering amplitude, eikonal approximations for nucleons will be introduced.

Let us consider two spinless nucleons, a and b, interacting via the exchange of vector mesons. Momenta of incident and final nucleons are denoted by p_j and p_j' (j=a and b), and those of emitted n pions by k_j (j=1,2,$\cdots$,n). Then the S-matrix element, which corresponds to the production diagram mentioned in §1, can be expressed as follows ;

$$\langle p_a', p_b'; k_1, \cdots, k_n | S | p_a, p_b \rangle = \langle f | S | i \rangle$$

$$= \langle f | T^* \cdot \exp \left[\int d^4x \int d^4y \, J_\mu^a(x) \left[\mathcal{L}_{\mu\rho}(x,y) + \mathcal{L}^0_{\mu\rho}(x,y) \right] J_\rho^b(y) \right] | i \rangle . \tag{2.1}$$

The nucleon currents $J_\mu^j(x)$, j=a and b, are given by the equations,

$$J_\mu^j(x) = i f^j \int d^4z \left[\psi_j^+(z) \cdot \frac{\partial}{\partial z_\mu} \psi_j(z) - \frac{\partial}{\partial z_\mu} \psi_j^+(z) \cdot \psi_j(z) \right] F(z-x), \tag{2.2}$$

where $\psi_j(x)$ stands for the nucleon field and f^j is the coupling constant between the j-nucleon and the vector meson. In order to keep generality, we include the nucleon form factor F(z-x). The appearance of T^*, not T ordered product, is originated from the

derivative coupling. The interaction term $\mathcal{L}_{\mu\rho}(x,y)$, which corresponds to the chain shown in Fig.1(a), is

$$\mathcal{L}_{\mu\rho}(x,y) = -ig\int d^4z\ D^V_{\mu\nu}(x-z)\,\varphi(z)\,D^V_{\nu\rho}(z-y). \tag{2.3}$$

Here, the pion field $\varphi(z)$ means the creation and annihilation of one pion, and g is the coupling constant between pion and vector mesons, The $D^V_{\mu\nu}(x-y)$ denotes the Feynman propagator of vector meson with mass m.

The second interaction term $\mathcal{L}^0_{\mu\rho}(x,y)$

$$\mathcal{L}^0_{\mu\rho}(x,y) = -D^V_{\nu\rho}(x-y) \tag{2.4}$$

is added, which means that the vector meson connects with two nucleons without emitting any pions. This term has been used to get the generalized crossed ladder diagrams in the previous paper[8].

After Abarbanel and Itzykson[7], we introduce here external C-number fields, $A^a_\mu(x)$ and $A^b_\rho(y)$, that can interact with nucleon currents. Then, with the aid of the functional derivatives, Eq.(2.1) may be rewritten in the form :

$$\langle f|S|i\rangle = \lim_{\substack{A^a\to 0\\ A^b\to 0}} \langle k_1,\cdots,k_m|\,\mathbb{C}_m\,|0\rangle\,\langle p'_a|\,\$_a\,|p_a\rangle\,\langle p'_b|\,\$_b\,|p_b\rangle, \tag{2.5}$$

where

$$\langle k_1,\cdots,k_m|\,\mathbb{C}_m\,|0\rangle = \langle k_1,\cdots,k_m|\,T\cdot\exp\Big[-\int d^4x\int d^4y\ \frac{\delta}{\delta A^a_\mu(x)}\big[\mathcal{L}_{\mu\rho}(x,y)+\mathcal{L}^0_{\mu\rho}(x,y)\big]\times\frac{\delta}{\delta A^b_\rho(y)}\Big]\,|0\rangle \tag{2.6}$$

and

$$\langle p' | \mathcal{S} | p \rangle = \langle p' | T^{*} \exp\left[i \int d^{4}x \, J_{\mu}(x) A_{\mu}(x) \right] | p \rangle . \tag{2.7}$$

The physical meaning of these terms is clear[8]. Especially, $\langle p' | \mathcal{S} | p \rangle$ in Eq.(2.7) represents the scattering of the nucleon in the external field $A_{\mu}(x)$ with non-local interaction.

At this stage, we introduce the eikonal approximation with respect to nucleon trajectories. This approximation corresponds to the straight going assumption of the nucleon in the course of scattering and reaction processes. This assumption might be thought as a good approximation at sufficiently high energies. This is because the experimental results for final momentum distribution of incident particle show a peak near the initial momenta, which is known as an incident particle effect.

The eikonal approximation used here consists of equating the momentum of the intermediate nucleon with the average value of initial and final momenta $\bar{p} = (p+p')/2$ [7]. In this approximation, the phase accumulation of incident wave occurs under the influence of the external field $A_{\mu}(x)$. The explicit form of the eikonalized S-matrix is given as follows, cf. Eq.(2.21) in the reference (8)*),

---

*) Here is a trivial difference from Eq.(2.21) in the previous paper[8], because non-local interaction is included in this paper.

$$\langle p' | S_e - 1 | p \rangle$$

$$= \frac{1}{\Pi \Pi'} \lim_{\alpha \to 0} \frac{d}{d\alpha} \int d^4x \; e^{i(p-p')x} \exp\left[-i \int_{-\infty}^{\alpha} d\tau \; V(x + 2\bar{p}\tau ; \bar{p})\right], \tag{2.8}$$

where

$$\Pi = \sqrt{2 p_0 (2\pi)^3} \quad , \quad \Pi' = \sqrt{2 p_0' (2\pi)^3} \tag{2.9}$$

and

$$V(x + 2\bar{p}\tau ; \bar{p}) = 2f \int d^4x' \; \bar{P}_\mu F(x + 2\bar{p}\tau - x') \; A_\mu(x'). \tag{2.10}$$

Substituting Eq.(2.8) into Eq.(2.5) and performing the functional derivatives, we obtain the following S-matrix element.

$$\langle f | S_e - 1 | i \rangle = \frac{1}{\Pi_a \Pi_{a'}} \frac{1}{\Pi_b \Pi_{b'}} \lim_{\substack{\alpha \to 0 \\ \beta \to 0}} \frac{d^2}{d\alpha d\beta} \int d^4x \int d^4y \; e^{i(p_a - p_{a'})x} \; e^{i(p_b - p_{b'})y}$$

$$\times \langle k_1, \cdots, k_n | T \cdot \exp\left[4 \int_{-\infty}^{\alpha} d\tau \int_{-\infty}^{\beta} d\sigma \; \bar{P}_{a\mu} \left[\frac{mG}{g} \mathcal{L}_{\mu\rho}(x + 2\bar{p}_a\tau, \; y + 2\bar{p}_b\sigma) \right.\right.$$

$$\left.\left. + G^0 \mathcal{L}^0_{\mu\rho}(x + 2\bar{p}_a\tau, \; y + 2\bar{p}_b\sigma)\right] \bar{P}_{b\rho}\right] | 0 \rangle, \tag{2.11}$$

where

$$G = f^a f^b g/m \qquad \text{and} \qquad G^0 = f^a f^b \; . \tag{2.12}$$

The expectation value of the T-ordered product contained in Eq.(2.11) can be exactly evaluated, and is given by the following relations :

$$\langle f|S_e - 1|i\rangle = \frac{1}{\pi_a \pi_{a'}} \frac{1}{\pi_b \pi_{b'}} \frac{1}{(n!)^{1/2}}$$
$$\times \lim_{\substack{\alpha\to 0\\ \beta\to 0}} \frac{d^2}{d\alpha d\beta} \int d^4x \int d^4y \; e^{i(p_a - p_{a'})x} \; e^{i(p_b - p_{b'})y}$$
$$\times \left\{ \prod_{j=1}^{n} u(k_j; x, y; \alpha, \beta) \right\} \cdot \exp\left[U(x-y; \alpha, \beta) + U^0(x-y; \alpha, \beta) \right], \tag{2.13}$$

where

$$u(k; x, y; \alpha, \beta) = \frac{1}{\sqrt{2k_0 (2\pi)^3}} \int d^4z \; e^{-ikz} \; w(z; x, y; \alpha, \beta), \tag{2.14}$$

$$U(x-y; \alpha, \beta) = \frac{1}{2} \int d^4x' \int d^4y' \; w(x'; x, y; \alpha, \beta) \; D_F^s(x'-y')$$
$$\times \; w(y'; x, y; \alpha, \beta), \tag{2.15}$$

$$U^0(x-y; \alpha, \beta) = 4 G^0 \int_{-\infty}^{\alpha} d\tau \int_{-\infty}^{\beta} d\sigma \; \bar{p}_{a\mu} \mathcal{L}^0_{\mu\rho}(x + 2\bar{p}_a \tau, \; y + 2\bar{p}_b \sigma) \; \bar{p}_{b\rho}, \tag{2.16}$$

and

$$w(z; x, y; \alpha, \beta) = \frac{4mG}{g} \int_{-\infty}^{\alpha} d\tau \int_{-\infty}^{\beta} d\sigma \; \bar{p}_{a\mu} \left[\frac{\delta}{\delta \varphi(z)} \mathcal{L}_{\mu\rho}(x + 2\bar{p}_a \tau, \; y + 2\bar{p}_b \sigma) \right] \bar{p}_{b\rho}. \tag{2.17}$$

Propagator $D_F^s(x'-y')$ in Eq.(2.15) has been reduced from the contraction of the pion field $\varphi(z)$, and corresponds to an internal meson line in Fig.2. Physically, $U(x,y;\alpha,\beta)$ represents a type of potential, which consists of two chains and one pion propagator connecting them as shown in Fig.2(b). The nucleon propagator does not appear explicitly in this expression, because it is replaced by a simple δ-function denoting the nucleon propagation in consequence of the eikonal approximation, cf. Eq.(2.8). On the

other hand, the term $u(k_j ; x,y ; \alpha,\beta)$, Eq.(2.14), contains one chain and one external pion line with momentum k_j.

The dependence of U and U^0 on the coordinates x and y of two nucleons is only their difference (x-y), because it is obvious from the translational invariance. This fact can be seen explicitly by expressing these terms in the momentum representations. Therefore by introducing relative coordinates Z=(x-y) and barycentric ones (x+y)/2 of the nucleons, we can perform the integration about (x+y)/2, which gives the energy-momentum conservation. Thus, an invariant amplitude can be written as follows;

$$\langle f|T_e|i\rangle = \frac{i}{(n!)^{1/2}} \lim_{\substack{\alpha\to 0\\ \beta\to 0}} \frac{d^2}{d\alpha\, d\beta} \int d^4Z\, e^{i\Delta Z} \left\{ \prod_{j=1}^{n} u_0(k_j ; Z ; \alpha,\beta) \right\} \times \exp\left[U(Z;\alpha,\beta) + U^0(Z;\alpha,\beta) \right], \tag{2.18}$$

where

$$\Delta = (P_a - P_a' - P_b + P_b')/2, \tag{2.19}$$

and the pion emitting term $u_0(k_j ; x-y ; \alpha,\beta)$ is reduced from $u(k_j ; x,y ; \alpha,\beta)$ in Eq.(2.14) by taking out the (x+y) dependent term, which shares the pion part of the energy-momentum conservation. Then this term u_0 depends only on the relative nucleon coordinates Z=(x-y). This invariant amplitude can be simplified by introducing new variables (b_x, b_y, ξ, ζ), which are related with Z by a relation $Z = b + 2\bar{p}_a\xi - 2\bar{p}_b\zeta$. The direction of z-axis is chosen to be pararell to $(\bar{P}_a - \bar{P}_b)$, and the two dimensional coordinates $\mathbf{b}$ are perpendicular to it. The Jacobian due to this

transformation is denoted by J,

$$J = 4 \left| \bar{P}_{a0} \bar{P}_{bz} - \bar{P}_{b0} \bar{P}_{az} \right| . \tag{2.20}$$

By the aid of this transformation, we arrive at the final form of the invariant amplitude.

$$\langle P'_a, P'_b ; k_1, \cdots, k_n | T_e | P_a, P_b \rangle$$
$$= \frac{i}{(n!)^{1/2}} J \int d^2 b \, e^{i \Delta \cdot b} \left[\left\{ \prod_{j=1}^{n} \Phi(b; k_j) \right\} e^{i\chi(b)} - \delta_{n0} \right] . \tag{2.21}$$

This form for the production amplitude is the same obtained previously by others[3),4)]. In our case, production factor $\Phi(b; k)$ and eikonal phase shift $\chi(b)$ can be reduced formally form Eqs.(2.14) to (2.17) by equating α and β with positive infinity and by replacing (x-y) with b:

$$\Phi(b; k) = U_0(k; b ; \alpha = \infty , \beta = \infty) \tag{2.22}$$

and

$$\chi(b) = -i \left[U(b; \alpha = \infty , \beta = \infty) + U^{\circ}(b; \alpha = \infty , \beta = \infty) \right] . \tag{2.23}$$

In the momentum space, these can be expressed as follows.

$$\Phi(b; k) = -im \frac{G}{(2\pi)^2} \int d^4 q \, e^{iq \cdot b} \, \delta[\bar{P}_a (q - \tfrac{1}{2} k)] \, \delta[\bar{P}_b (q + \tfrac{1}{2} k)]$$
$$\times \bar{P}_{a\mu} F((q - \tfrac{1}{2} k)^2) \, \frac{\delta_{\mu\nu} + (q - \tfrac{1}{2} k)_\mu (q - \tfrac{1}{2} k)_\nu / m^2}{(q - \tfrac{1}{2} k)^2 + m^2}$$
$$\times \frac{\delta_{\nu\rho} + (q + \tfrac{1}{2} k)_\nu (q + \tfrac{1}{2} k)_\rho / m^2}{(q + \tfrac{1}{2} k)^2 + m^2} F((q + \tfrac{1}{2} k)^2) \, \bar{P}_{b\rho} . \tag{2.24}$$

and

$$\chi(b) = -\frac{1}{2(2\pi)^4}\int d^4k\ \frac{\Phi(b;k)\ \Phi(b;-k)}{k^2+\mu^2-i\epsilon}$$

$$+\frac{G^0}{(2\pi)^2}\int d^4q\ \delta(\bar{P}_a q)\ \delta(\bar{P}_b q)$$

$$\times \bar{P}_{a\mu} F(q^2)\frac{\delta_{\mu\rho}+q_\mu q_\rho/m^2}{q^2+m^2}F(q^2)\bar{P}_{b\rho}\, e^{iqb} \qquad (2.25)$$

The mass dependent term in the numerator of vector meson propagator vanishes exactly because of δ-functions. Furthermore, it is easily proven from Eq.(2.24) that $\Phi(b;k)$ has the following property.

$$\Phi(b;k) = -\Phi^*(b;-k) = \Phi(-b;-k). \qquad (2.26)$$

By the aid of the last relation, the real and imaginary parts of the eikonal phase shift defined by

$$\chi(b) = \chi_r(b) + i\,\chi_i(b) \qquad (2.27)$$

are given as follows :

$$\chi_i(b) = \frac{1}{2}\int\frac{d^3k}{2k_0(2\pi)^3}|\Phi(b;k)|^2 \qquad (2.28)$$

and

$$\chi_r(b) = \frac{1}{2}P\int\frac{d^4k}{(2\pi)^4}\ \frac{|\Phi(b;k)|^2}{k^2+\mu^2}$$

$$+\frac{G^0}{(2\pi)^2}\frac{4\bar{P}_a\bar{P}_b}{J}\int d^2q_\perp\, F(q_\perp^2)\frac{1}{q_\perp^2+m^2}F(q_\perp^2)\,e^{iq_\perp\cdot b}, \qquad (2.29)$$

where $\not{q}_\perp$ stands for the two dimensional vector lying in the $\not{b}$-plane.

In general, from unitarity requirement, the eikonal phase shift must have its positive imaginary part, which is reduced from an absorption of incident wave into many open inelastic channels. In the present case, the imaginary eikonal phase shift has been explicitly derived, not phenomenologically, by specifying the mechanism of production process. Moreover, functional form of the phase shift is determined on the bases of the covariant field theory.

The relation between $\chi_i(b)$ and $\Phi(\not{b}\,;\,k)$ was firstly discovered by Calucci, Jengo and Rebbi[3]. However, their treatment is non-covariant, and their functional forms of $\Phi(\not{b}\,;\,k)$, and hence of $\chi_i(b)$, are left undetermined. Thus far, no approximations are performed other than the eikonal approximation applied on the high energy nucleons. As seen from Eq.(2.21), our invariant amplitude is written as the integration over the two dimensional vector $\not{b}$. It is considered as a generalization of the impact parameter expansion to the production process.

§3 Expressions for observable quantities

In this section, by introducing some kinematical approximations, various quantities obtained in the previous section will be rewritten into more compact forms. In addition, physically observed quantities will be expressed by $\Phi(\mathbf{b};k)$ and $\chi(b)$. It is also shown that the present theory satisfies the s-channel unitarity.

In order to see the physical features explicitly, it will be assumed that produced pions have not large energy, and are emitted nearly symmetrically in forward and backward directions; namely we shall neglect the terms of order $k_0/\sqrt{s}$ and $(\Sigma\mathbf{k})/\sqrt{s}$ in comparison with the leading terms.

First, features of $\Phi(\mathbf{b};k)$ will be considered. The momentum q_z and the energy q_0 of the virtual vector meson are limited to the definite values through two δ-functions in Eq.(2.24). Within our approximations stated above, they are

$$q_z \cong -\frac{1}{2\beta} k_0 \quad \text{and} \quad q_0 \cong -\frac{\beta}{2} k_z , \tag{3.1}$$

where

$$\beta = \frac{\bar{P}_{az} - \bar{P}_{bz}}{\bar{P}_{a0} + \bar{P}_{b0}} . \tag{3.2}$$

Therefore, integrations over q_z and q_0 can be done and the following expressions for $\Phi(\mathbf{b};k)$ is obtained

$$\Phi(\mathbf{b};k) = im \frac{G}{(2\pi)^2} \int d^2\mathbf{q}_\perp \, e^{i\mathbf{q}_\perp\cdot\mathbf{b}} \times \frac{F((q-\frac{1}{2}k)^2)}{(q-\frac{1}{2}k)^2 + m^2} \frac{F((q+\frac{1}{2}k)^2)}{(q+\frac{1}{2}k)^2 + m^2} . \tag{3.3}$$

In the last expression, because of Eq.(3.1), we have

$$(q \pm \tfrac{1}{2}k)^2 = (q_\perp \pm \tfrac{1}{2}k_\perp)^2 + \frac{1}{4\gamma^2}\left(k_z \mp \frac{1}{\beta}k_0\right)^2, \tag{3.4}$$

with

$$\gamma = 1/\sqrt{1-\beta^2} \tag{3.5}$$

An appearance of γ-factor represents physically the Lorentz contraction of each cloud of nucleons in the center of mass system. It has a strong relation to the Feynman scaling for the inclusive spectra of emitted pions, as will be shown later.

It might be worthy of notice that this Lorentz factor has been reduced out as a natural consequence of model calculations based on the covariant field theory, without inputting it as an extra condition.

As is easily checked from Eq.(3.3), $\Phi(b;k)$ has following properties besides one given by Eq.(2.26).

$$\Phi(b;k_\perp, k_0) = \Phi(b;-k_\perp, k_0) \tag{3.6}$$

and

$$\Phi(b;k_\perp, k_0) = -\Phi^*(b;k_\perp, -k_0) \tag{3.7}$$

The real and imaginary parts of the eikonal phase shift are ultimately determined through the combinations of $\Phi(b;k)$ with Eqs.(2.28) and (2.29).

Since invariant amplitude has been obtained in a closed form. physically observed quantities can be calculated at least in principle by using Eq.(2.21). In the present model, some of them take fairly simple expressions. We should like to list up a few examples without proof:

Inclusive spectra for the emitted pions:

$$k_0 \frac{d\sigma}{d\mathbf{k}} = \frac{1}{2(2\pi)^3} \int d^2\mathbf{b}\, |\Phi(\mathbf{b};k)|^2 \tag{3.8}$$

Total cross section:

$$\sigma_T = 2 \int d^2\mathbf{b}\, [1 - e^{-\chi_i(b)} \cos \chi_r(b)] \tag{3.9}$$

Elastic total cross section:

$$\sigma_0 = \int d^2\mathbf{b}\, [1 + e^{-2\chi_i(b)} - 2 e^{-\chi_i(b)} \cos \chi_r(b)] \tag{3.10}$$

Cross section for the production of n pions:

$$\sigma_n = \frac{1}{n!} \int d^2\mathbf{b}\, [2\chi_i(b)]^n e^{-2\chi_i(b)} \tag{3.11}$$

Average multiplicity for emitted pions normalized to the inelastic total cross section $\sigma_{in} = \sigma_T - \sigma_0$:

$$\langle n \rangle = \frac{2}{\sigma_{in}} \int d^2\mathbf{b}\, \chi_i(b) \tag{3.12}$$

Elastic differential cross section:

$$\frac{d\sigma}{dt} = \pi \left| \int_0^\infty b\,db\, J_0(b\sqrt{-t})[1 - e^{i\chi(b)}] \right|^2, \tag{3.13}$$

where $t = -(p_a - p_a')^2$.

Since b-integrations in Eq.(3.8) can be easily performed as clear from $\Phi(\mathbf{b};k)$ in Eq.(3.3), inclusive spectra take specially simple expressions, see Eq.(4.5). In our model, production cross section σ_n is expressed as a superposition of the Poisson distribution.

As far as an invariant amplitude is expressed in the form given

by Eq.(2.21) with an arbitrary function for the production factor $\Phi(\mathbf{b};k)$, the s-channl unitarity requires three conditions on the functional property of $\Phi(\mathbf{b};k)$. Two of them are Eqs.(2.26) and (3.6), and the other is

$$\underline{\Phi}(\mathbf{b};k) = \underline{\Phi}(-\mathbf{b};k) \tag{3.14}$$

Our $\Phi(\mathbf{b};k)$ in Eq.(3.3) does not satisfy the last condition. However, we would like to point out that our invariant amplitude is consistent with the s-channel unitarity for the elastic case.

$$\frac{1}{2i}\langle P_a', P_b'|T_e - T_e^+|P_a, P_b\rangle$$

$$= -\frac{(2\pi)^4}{2}\sum_{P'',k'',n}\delta^4\left(P_a'' + P_b'' + \sum_{j=1}^{n} k_j'' - P_a - P_b\right)$$

$$\times \langle P_a', P_b'|T_e^+|P_a'', P_b'', k_1'', \cdots, k_n''\rangle\langle P_a'', P_b'', k_1'', \cdots, k_n''|T_e|P_a, P_b\rangle \tag{3.15}$$

In this case, the necessary condition on $\Phi(\mathbf{b};k)$ is only Eq.(3.6).

§4 Comparison with experiments

Our theoretical results will be compared with the proton-proton collision data. We proceed as follows. Though our model ignores completely isospin variables, experimental data on the inclusive spectra of positive pions are used to fix the nucleon form factor and two undetermined parameters, namely, coupling constant G and virtual vector meson mass m. With these parameters, it will be investigated to what extent our theoretical predictions reproduce other experimental results, especially elastic scattering data. These procedures may be the measure of the importance of the production mechanism assumed here.

First, as the functional form of $F(k^2)$, which represents the non-local interaction of nucleon with the vector meson, we assume the following form,

$$F(k^2) = \left(\frac{m^2}{k^2 + m^2}\right)^{\nu}. \tag{4.1}$$

Furthermore, the mass in $F(k^2)$ will be identified, not necessarily at all, with our vector meson mass, because the use of two different masses merely causes an increace of the number of parameters.

Now, the production factor $\Phi(\mathbf{b};k)$ and the eikonal phase shift $\chi(b)$ have following expressions.

$$\Phi(\mathbf{b};k) = i\frac{G}{(2\pi)^2} m^{4\nu+1} \int d^2q_\perp \, e^{i\mathbf{q}_\perp\cdot\mathbf{b}} \times \left[\frac{1}{(q-\frac{1}{2}k)^2+m^2}\right]^{\nu+1}\left[\frac{1}{(q+\frac{1}{2}k)^2+m^2}\right]^{\nu+1}, \tag{4.2}$$

$$X_i(b) = \frac{1}{2}\int \frac{d^3k}{2k_0(2\pi)^3} |\Phi(b;k)|^2, \tag{4.3}$$

and

$$X_R(b) = \frac{1}{2} P\int \frac{d^4k}{(2\pi)^4} \frac{|\Phi(b;k)|^2}{k^2 + \mu^2} - \frac{G^0}{2\pi} \frac{1}{(2\nu)!} \left(\frac{mb}{2}\right)^{2\nu} K_{2\nu}(mb), \tag{4.4}$$

where $K_{2\nu}(z)$ is the 2ν-th modified Bessel function of the second kind.

The analytic form for the inclusive pion spectra is derived from Eq.(3.8), that is,

$$k_0 \frac{d\sigma}{d\vec{k}} \equiv F(k_\perp, k_z, s) = \left[\frac{G}{2(2\pi)^2} m^{4\nu+1}\right]^2 \int d^2q_\perp \left[\frac{1}{(q_\perp - \frac{1}{2}k_\perp)^2 + d_+} \frac{1}{(q_\perp + \frac{1}{2}k_\perp)^2 + d_-}\right]^{2\nu+2}, \tag{4.5}$$

where

$$d_\pm = \frac{1}{4\gamma^2}\left(k_z \pm \frac{1}{\beta} k_0\right)^2 + m^2. \tag{4.6}$$

By introducing a Feynman parameter to combine two denominators, the momentum integral can be performed, and the inclusive spectra become

$$F(k_\perp, k_z, s) = \frac{1}{2}\left[\frac{G}{2(2\pi)^2} m^{4\nu+1}\right]^2 \frac{(4\nu+2)!}{[(4\nu+2)!!]^2} \times \int_{-1}^{1} dy \frac{(1-y^2)^{2\nu+1}}{\left[D + y\frac{k_0 k_z}{\beta\gamma^2} - y^2\frac{k_\perp^2}{4}\right]^{4\nu+3}}, \tag{4.7}$$

where

$$D = \frac{1}{4\gamma^2}\left(k_z^2 + \frac{1}{\beta^2}k_0^2\right) + \frac{1}{4}k_\perp^2 + m^2. \qquad (4.8)$$

These expressions show that the pion inclusive spectra has a scaling behavior. The integrand of Eq.(4.7) has a sharp peak around $y \simeq 0$. Thus, it can be expected that the features of $F(k_\perp, k_z, s)$ is mainly determined by the first term in the denominator, D. Consequently, when the incident energy becomes sufficiently large, we have little contribution from terms which depend on s explicitly, and the inclusive spectra is

$$F(k_\perp, k_z, s) \longrightarrow f\left(k_\perp, x = \frac{1}{M}\left(\frac{k_z}{\gamma}\right)\right) \qquad (4.9)$$

Thus the Feynman scaling behavior is established, as expected from our assumption on the production mechanism. M is the nucleon mass.

Comparison with experimental data on the inclusive spectra at $p_{lab} = 19.2$ [GeV/c] by Allaby et al. are shown in Fig.4. Parameters are chosen to be $m^2 = 0.47[(\mathrm{GeV}/c^2)^2]$, $G/(2\pi)^2 = 28.4$, and $\nu = 2$. This selection $\nu = 2$ corresponds to the case where the experimentally observed electromagnetic form factor is adopted for the nucleon cloud. (If ν is set equal to zero, namely $F(k^2) = 1$, mass of the vector meson must be chosen very small so as to reproduce the inclusive spectra.)

The qualitative features of the inclusive spectra are reproduced fairly well; namely, the $k_\perp$ and $k_{/\!/}$ spectra have maximums at $k = 0$, respectively, and the $k_{/\!/}$ distribution is flatter than the $k_\perp$ one. The latter features are due to the existence of

the γ-factor combined with $k_{//}$.

Next, let us consider the eikonal phase shift $\chi(b)$. The real part $\chi_r(b)$ is necessary to determine the ratio of the real to imaginary part of the elastic amplitude at t=0. But experimental data show that the ratio is small. Actually, $\chi_r(b)$ given by Eq.(4.4) contains another undetermined parameter G^0, and we could make $\chi_r(b)$ negligibly small by choosing it appropriately. Therefore, the real part $\chi_r(b)$ is neglected hereafter. Then our scattering amplitude becomes pure imaginary. The numerical value of the imaginary part of eikonal phase shift, $\chi_i(b)$, is uniquely predicted by using the values of m^2 and G determined from the inclusive spectra. As we have to perform multiple integrals to get this prediction, we used the Monte-Carlo method. We believe that our error for computational results is within 5% at the largest. The results are shown by the solid lines in Fig.5 for $\chi_i(b)$ and the function $\Gamma(b)= 1-\exp[-\chi_i(b)]$. The b-dependence of our eikonal phase shift is so similar to the Gaussian distribution, $\exp(-b^2/b_0^2)$.

For comparison, in Fig.5 are shown the b-dependence of the eikonal phase shift given by Durand and Lipes[10], namely*),

$$\chi_i(b) = A\left(\frac{\mu b}{2}\right)^3 K_3(\mu b). \qquad (4.10)$$

---

*) We choose $\mu^2=0.98[(\mathrm{GeV}/c^2)^2]$ and A=1.82 to give the same total cross section and the same slope parameter as in our calculation. These selection seem to reproduce a nice fit to the experimental $d\sigma/dt$.

This form for $\chi_i(b)$ is proposed by them to reproduce the experimental results on the p-p elastic collision, according to the Chou and Yang conjecture.[11)]

Since the numerical values of our $\chi_i(b)$ are obtained, let us return to compare our theoretical predictions with experimental data. The total cross section, σ_T in Eq.(3.9), is estimated to be

$$\sigma_T = 39.1 [\text{mb}], \tag{4.11}$$

which is in nice agreement with experiment.

The calculated $d\sigma/dt$ is plotted in Fig.6, together with some experimental points by Allaby et al.[12)] Agreements with the data are fairly well in the small $|t|$ regions. For example, the slope parameter b is 9.50 $[(\text{GeV/c})^{-2}]$, which is estimated between $|t| = 0$ and 0.05. The gloval slope up to $t = -0.7$ is, however, slightly steeper than the experimental one, and so the first dip appears at $t = -0.95$, though experimentally at $t = -1.3$**). Though the theoretical $d\sigma/dt$ seems to have more structure than the experimentally observed, this difference might be partially due to the neglection of the real part of the eikonal phase shift in our numerical calculations.

The elastic total cross section σ_0 is 8.05 [mb] in our case. Then, its ratio to the total cross section is

$$\sigma_0/\sigma_T = 0.21 \quad \text{at } p_{lab} = 19.2 \text{ [GeV/c]}: \tag{4.12}$$

**) Although recent I.S.R. data[15)] exhibit a steeper slope than ours, a dip appears at $t = -1.4$.

which seems to be fairly well.

The theoretical results on σ_n are tabulated in Table.1, and the maximum appears at n = 1. The average multiplicity <n> is estimated to be

$$<n> = 1.71. \tag{4.13}$$

Since we do not take the isotopic spin into account, we can not say definitely about the charged states of pions. It may, however, be allowed to assume that the number of charged pions in our calculation should be multiplied by 2, though there must be the positive pion excess for p-p collisions. For comparison, the experimental cross sections[13),14)] σ_n(ch) for both positive and negative charged pions at p_{lab} = 18.9 [GeV/c] are also shown in Table.1. The average multiplicity is $<n^{(ch)}> = 3.7 \pm 0.5$. We may say that agreements are fairly well. It remains unsolved how to include the isospin in the treatment of the eikonal approximation.

§5 Conclusions and Discussions

Some successful results have been obtained by assuming the special production mechanism.

As one of them, the Feynman scaling behavior for inclusive spectra of the emitted pions is automatically derived in our model, as mentioned in §4. The essential points are the use of the covariant field theory, the choice of vector meson as an exchange particle, the eikonal approximation about nucleon trajectories, and the special assumption for the production mechanism. Especially, it is crucial to have assumed one pion production from one chain in Fig.1(a). As a result of this assumption, the information that each of nucleons is going straightforward, is sent to this produced pion directly from these nucleons. Mathematically, this is expressed in such a way that the momentum of one emitted pion appears commonly in the arguments of two δ-functions in the production factor $\Phi(\mathbf{b}; k)$, Eq.(2.24). On the other hand, if two or more pions are emitted from one chain like in Fig.1(b) and (c), these circumstances do not occur; therefore we cannot expect the Feynman scaling to be derived without any additional assumptions.

Concerning the inclusive spectra itself, general tendencies found in experiments are well reproduced in the pionization regions. There seems, however, to be disagreement in the small $k_\perp$ domains. That is, it can be seen not only from the flattened peak of the distribution near $k_\perp=0$ in Fig.4(b), but also from lower theoretical values of the $k_{/\!/}$ distribution for the fixed $k_\perp=0.2$ in Fig.4(a).

These defects may be remedied by modifying our production mechanism, in which the emission of two or more pions from one chain, Fig.1(c) and so on, is not considered. Furthermore, there are apparent discrepancy in the large $k_{//}$ domain. This may be because the production process due to the direct pion emission from nucleons, the so-called fragmentation, are not taken into account. The estimation of the contribution from these additional production mechanism should be done in future[20)]

The imaginary part of the eikonal phase shift reproduces well the diffractive properties in elastic differential cross sections, in spite of assuming the simple production mechanism and neglecting the fragmentation process. Our imaginary part is a reflection of the s-channel unitarity, in contrast with the Regge pole theory which asserts that the t-channel unitarity governs the high energy behavior in the s-channel. Quantitatively, slightly steeper a slope for diffraction peak and a dip at rather small $|t|$ value are obtained. The similar shape has been gained by the Regge eikonal model[6)], where the Gaussian b-dependence of $\chi_i(b)$ is adopted. Its origin can be understood in terms of the features of $\chi_i(b)$. Since the better fit with experimental results for the diffraction peak has been obtained from $\chi_i(b)$ shown by dashed line in Fig.5, it seems to be preferable that $\chi_i(b)$ has larger value at b=0 and shorter range in its b-distribution. Such desirable features for $\chi_i(b)$ may be reduced from production processes in which more than one pion are emitted from one chain.

So as to see the essential features of our model, let us

assume a rough approximation that $\chi_i(b)$ is effectively replaced by a θ-function, $(A/2)\theta(b_0-b)$, under the condition

$$\frac{1}{2}Ab_0 = \int_0^\infty db\ \chi_i(b)\ . \tag{5.1}$$

Then observable quantities are expressed as follows.

$$\sigma_T = 2\pi b_0^2\ [1 - e^{-A/2}]\ , \tag{5.2}$$

$$\sigma_0 = \pi b_0^2\ [1 - e^{-A/2}]^2\ , \tag{5.3}$$

$$\sigma_n = \pi b_0^2\ \frac{A^n}{n!}\ e^{-A}\ , \tag{5.4}$$

and

$$\langle n \rangle = A\ [1 - e^{-A}]^{-1}\ . \tag{5.5}$$

It must be noted that our expression for the production amplitude makes it possible to relate different observables through only two parameters, A and b_0.

According to the experiments, the ratio σ_0/σ_T is about 0.24 at P_{lab}=19.2 [GeV/c]. From this ratio and Eqs.(5.2) and (5.3), the values of A is about 1.3, and then the average multiplicity becomes $\langle n \rangle \simeq 1.8$. It is interested to note that this vaue of $\langle n \rangle$ happens to be almost equal to our previous result, Eq.(4.13), while our numerical result for σ_0/σ_T, Eq.(4.12), was also consistent with the experimental data.

By judging from the comparisons of the present theory with experiments so far seen, our assumed production mechanism in the

pionization regions seems to reflect the part of the essential nature of high energy nucleon-nucleon collisions. However, it should be investigated what the energy dependences of $\langle n \rangle$ and σ_T are, and whether the inclusive spectra for the final protons are able to be reproduced or not. These problems will be discussed elsewhere.

Concerning more than one pion production from one chain, Koyama[17] has proposed general procedure to treat the production diagrams, in which all diagrams in Fig.1 and their s-channel repetition are included. On the other hand, Auerbach, Aviv, Sugar and Blankenbelcer[18], and Sugar[19] have widely investigated the j-plane nature of the scattering amplitude, which is obtained from the repetition of the multi-peripheral chains. In addition, it is an open question how to take into consideration of the resonance production and the fragmentation process[20),21] in the framework of the eikonal formalism.

Acknowledgement

The author would like to express his sincere thanks to Professor T. Kotani for helpful discussions and suggestions during this work. He is also grateful to Professor Y. Watanabe, who kindly lead him in performing the computational works, and Drs. S. Sasaki and H. Koyama for their useful comments and encouragements.

References

1) E. Leader and U. Maor, Phys. Letters 43B (1973), 505.
U. Amaldi, NP Internal Report 73-5, and references therein.

2) R. P. Feynman, Phys. Rev. Letters 23 (1969), 1415.

3) G. Calucci, R. Jengo and C. Rebbi, Nuovo Cim. 4A (1971), 330, 6A (1971), 601.

4) R. Aviv, R. L. Sugar and R. Blankenbecler, Phys. Rev. D5 (1972), 3252.

5) H. M. Freid, Phys. Rev. D6 (1972), 3562.

6) D. Amati, A. Stanghellini and S. Fubini, Nuovo Cim. 26 (1962), 896.
G. F. Chew and A. Pignotti, Phys. Rev. 176 (1968), 2112.
C. E. De Tar, Phys. Rev. D3 (1971), 128, and references therein.

7) H. D. I. Abarbanel and C. Itzykson, Phys. Rev. Letters 23 (1969), 53.

8) M. Doi and T. Kotani, Prog. Theo. Phys. 49 (1973), 242.

9) Allaby, Binon, Diddens, Duteil, Klovning, Meunier, Peigneux, Sacharidis, Schlümmann, Spighel, Stroot, Thorndike and Wetherell, CERN report 70-12 (1970).

10) L. Durand, III and R. Lipes, Phys. Rev. Letters. 20 (1968), 637.

11) T. T. Chou and C. N. Yang, Phys. Rev. 170 (1968), 1951.

12) Allaby, Binon, Diddens, Duteil, Klovning, Meunier, Peigneux, Sacharidis, Schlüpmann, Spighel, Stroot, Thorndike and Whetherell, Phys. Letters 28B (1968), 67.

13) F. F. Abraham and R. M. Kalbach, Nuovo Cim. 26 (1962), 717.

14) Boggild, Hansen and et al., Phys. Letters 30B (1969), 369.

15) Böhm, Bozzo, Ellis, Foeth, Ferrero, Maderni, Naroska, Rubbia, Sette, Staude, Strolin and de Zorzi, to be published.

16) S. Frautch and B. Margolis, Nuovo Cim. 56A (1968), 1155.
S. C. Frautchi, C. J. Hamer and F. Ravndal, Phys. Rev. D2 (1970), 2681.
C. J. Hamer and F. Ravndal, Phys. Rev. D2 (1970), 2687.

17) H. Koyama, to be published.

18) S. Auerbach, R. Aviv, R. Sugar and R. Blankenbecler, Phys. Rev. Letters 29 (1972), 522; Phys. Rev. D6 (1972), 2216.

19) R. L. Sugar, Phys. Rev. D8 (1973), 1134.

20) S. Tanaka, Phys. Rev. D4 (1971), 2419.

21) M.Doi, to be published.

Figure captions

Fig.1 Possible production diagrams from one chain. ——— for nucleon, ∿∿∿ for vector meson, and ----- for pion.

Fig.2 Examples of crossed ladder diagrams for the production mechanism assumed in this paper. Only the case of two pion emission is shown. All possible interchanges of the legs of chains along each nucleon lines should be taken.

Fig.3 Various interaction types corresponding to the diagrams in Fig.1(a). In these figures, V_μ and A_ν stand for the vector and pseudovector fields, respectively, and S is the spin of the nucleon. Pion field is psedoscalar in Figs.(a) and (b). In Fin.(c), both pion and nucleon are taken to be scalar.

Fig.4 Inclusive spectra for positive pions at p_{lab}=19.2 [GeV/c]. The experimental data are due to Allaby et al.[9].

Fig.5 The b-dependence of the imaginary part of the eikonal phase shift, $\chi_i(b)$, and of the function, $\Gamma(b)=1-\exp[-\chi_i(b)]$. Solid lines represent our numerical results. For comparison, those by Durand and Lipes[10] are also plotted by dashed lines.

Fig.6 Elastic differential cross section, $d\sigma/dt$. The theoretical result by the use of our $\chi_i(b)$ is drawn by the solid line. The experimental data at p_{lab}=19.2 [GeV/c] by Allaby et al.[12] are cited.

Table caption

Table 1 Theoretical results for the cross section σ_n as a function of pion multiplicity n. The experimental data on charged pions are taken from the reference (13). Experimental elastic total cross section σ_0 at p_{lab}= 19.0 [GeV/c] is quoted from the reference (14).

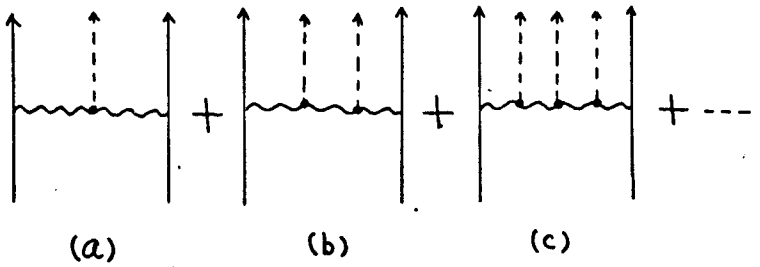

Fig. 1

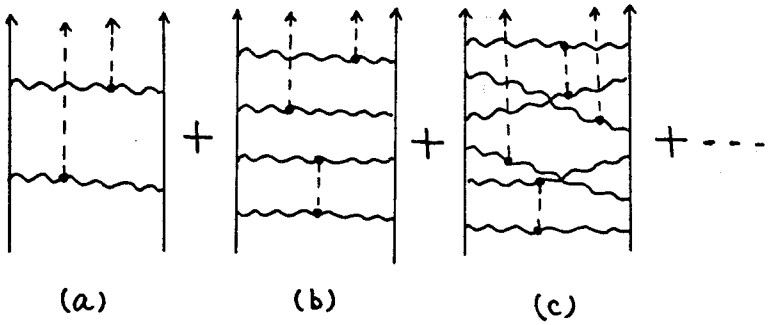

Fig. 2

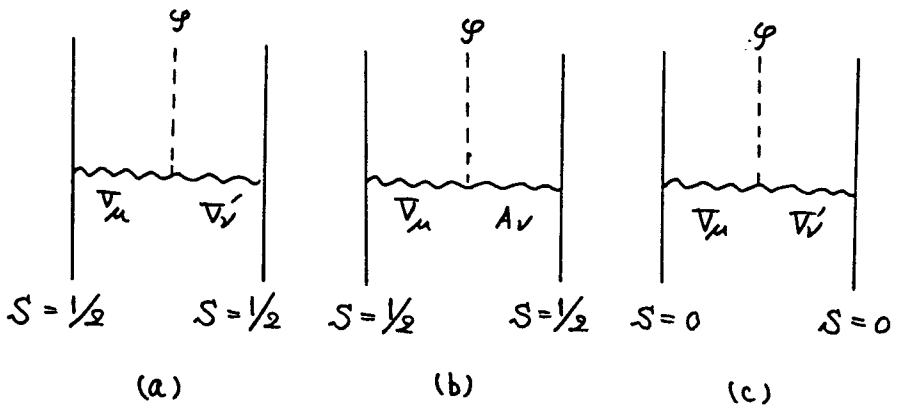

Fig. 3

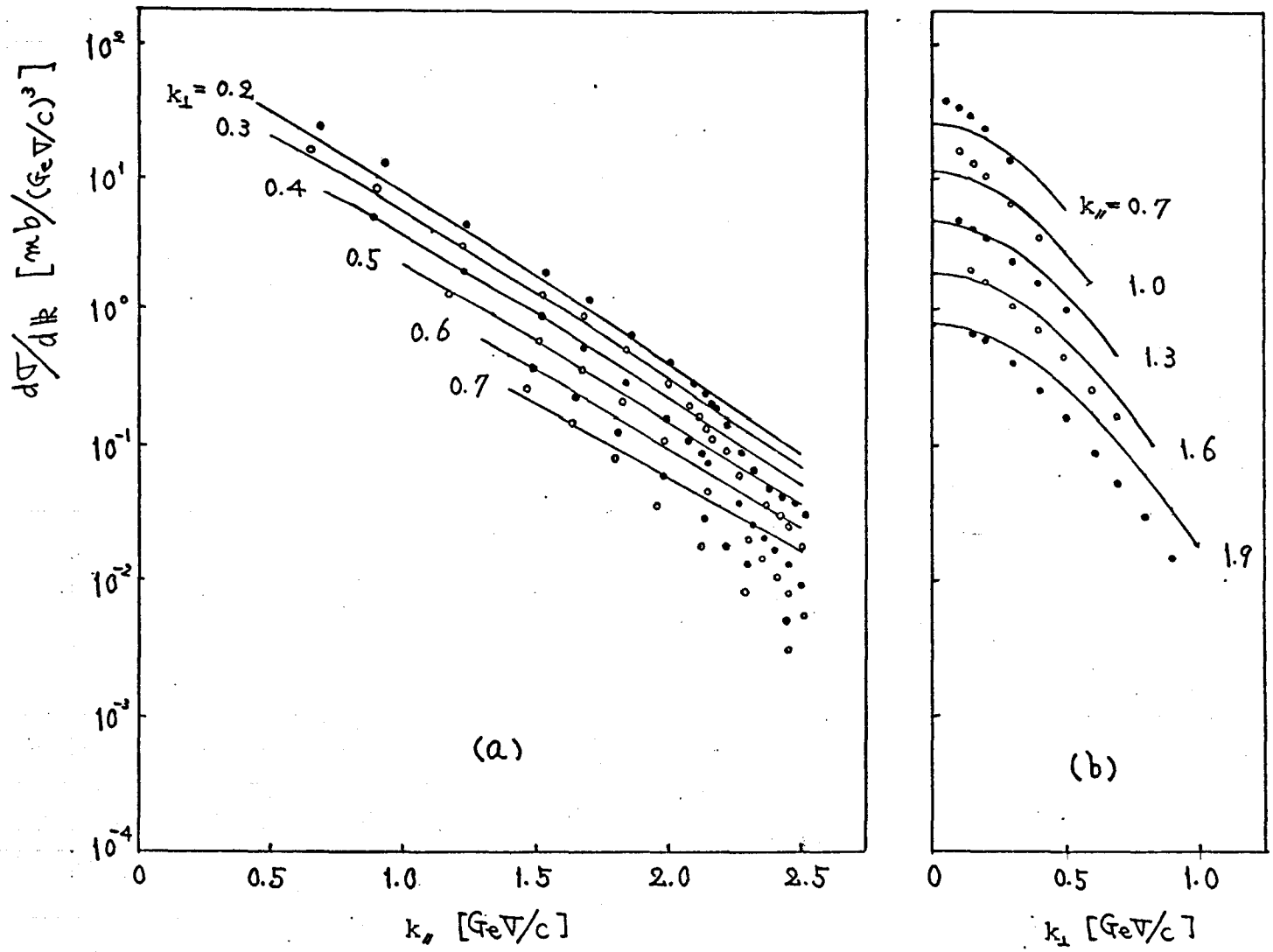
$d\sigma/dp_{\parallel}$ [mb/(GeV/c)^3]
10^2
10^1
10^0
10^{-1}
10^{-2}
10^{-3}
10^{-4}
$k_\perp$ = 0.2
0.3
0.4
0.5
0.6
0.7
(a)
0
0.5
1.0
1.5
2.0
2.5
$k_\parallel$ [GeV/c]
$k_\parallel$ = 0.7
1.0
1.3
1.6
1.9
(b)
0
0.5
1.0
$k_\perp$ [GeV/c]

Fig. 4

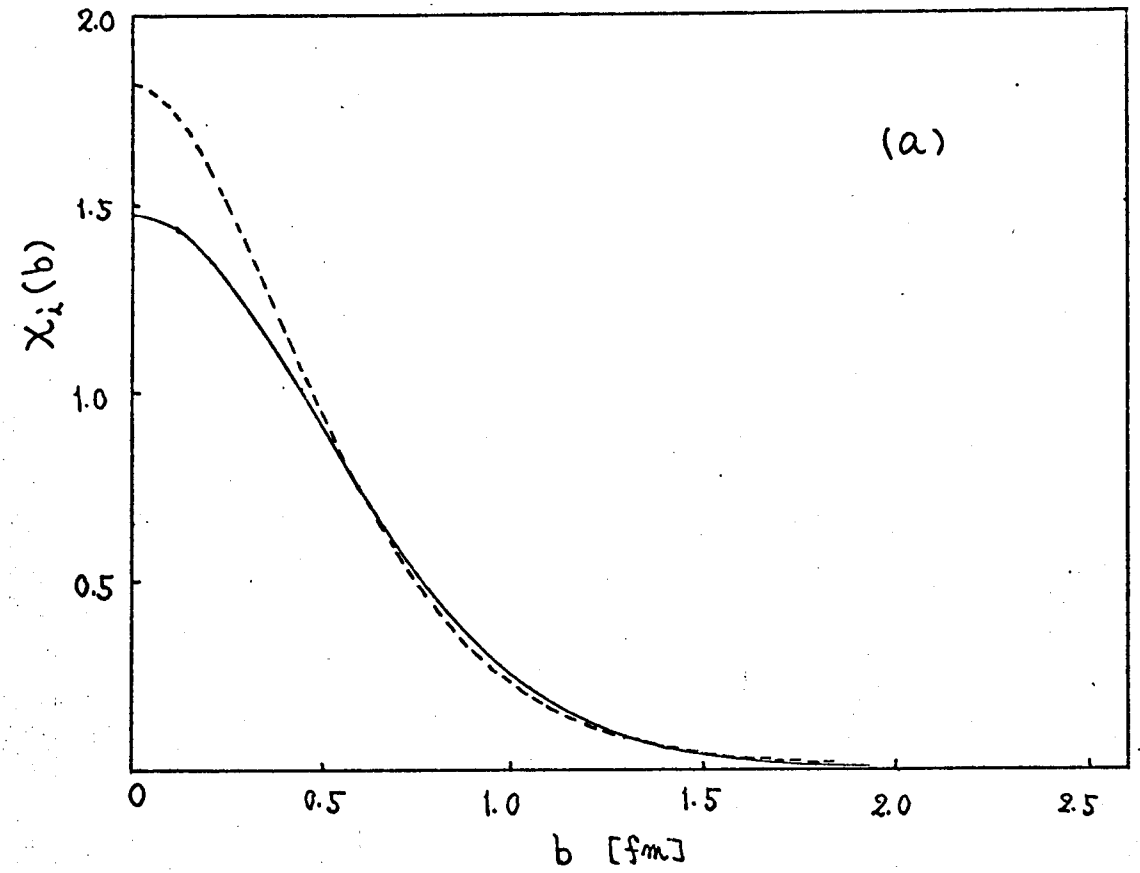
(a)
$\chi_i(b)$
2.0
1.5
1.0
0.5
0
0.5
1.0
1.5
2.0
2.5
b [fm]

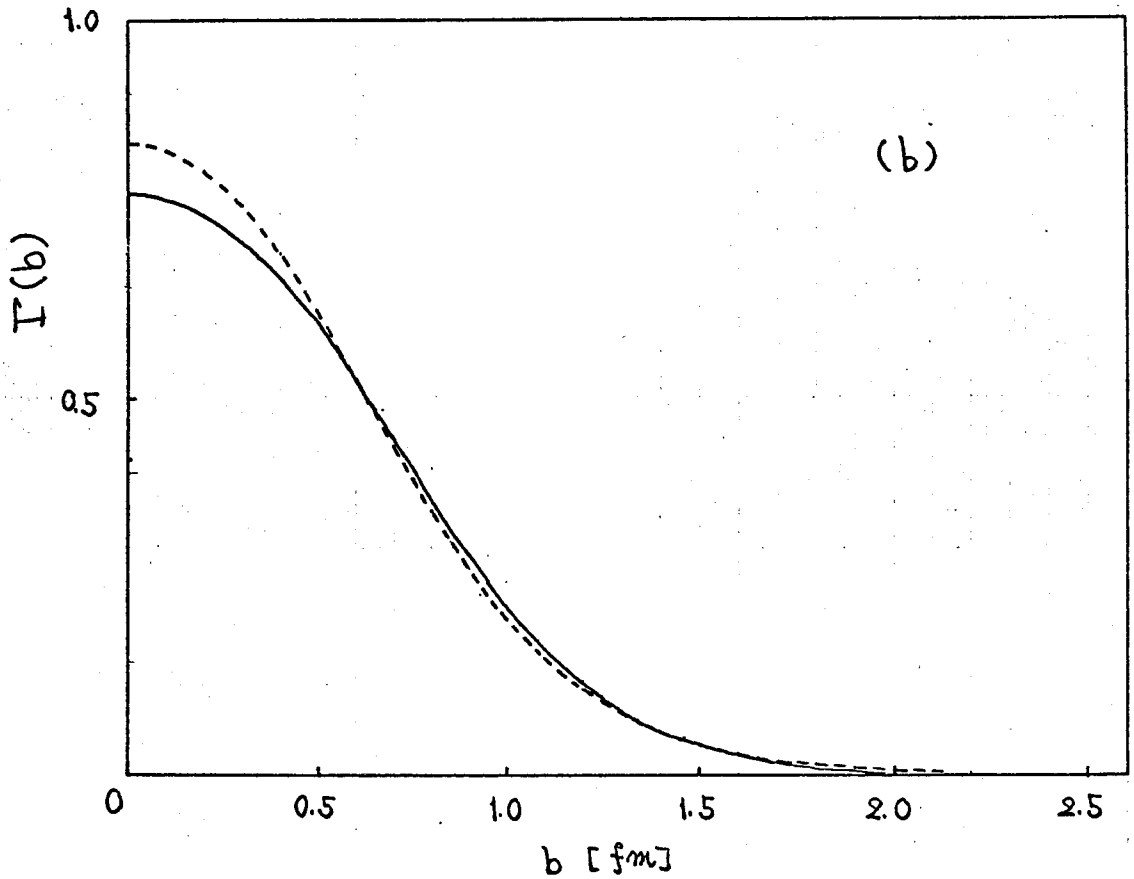
(b)
$\Gamma(b)$
1.0
0.5
0
0.5
1.0
1.5
2.0
2.5
b [fm]

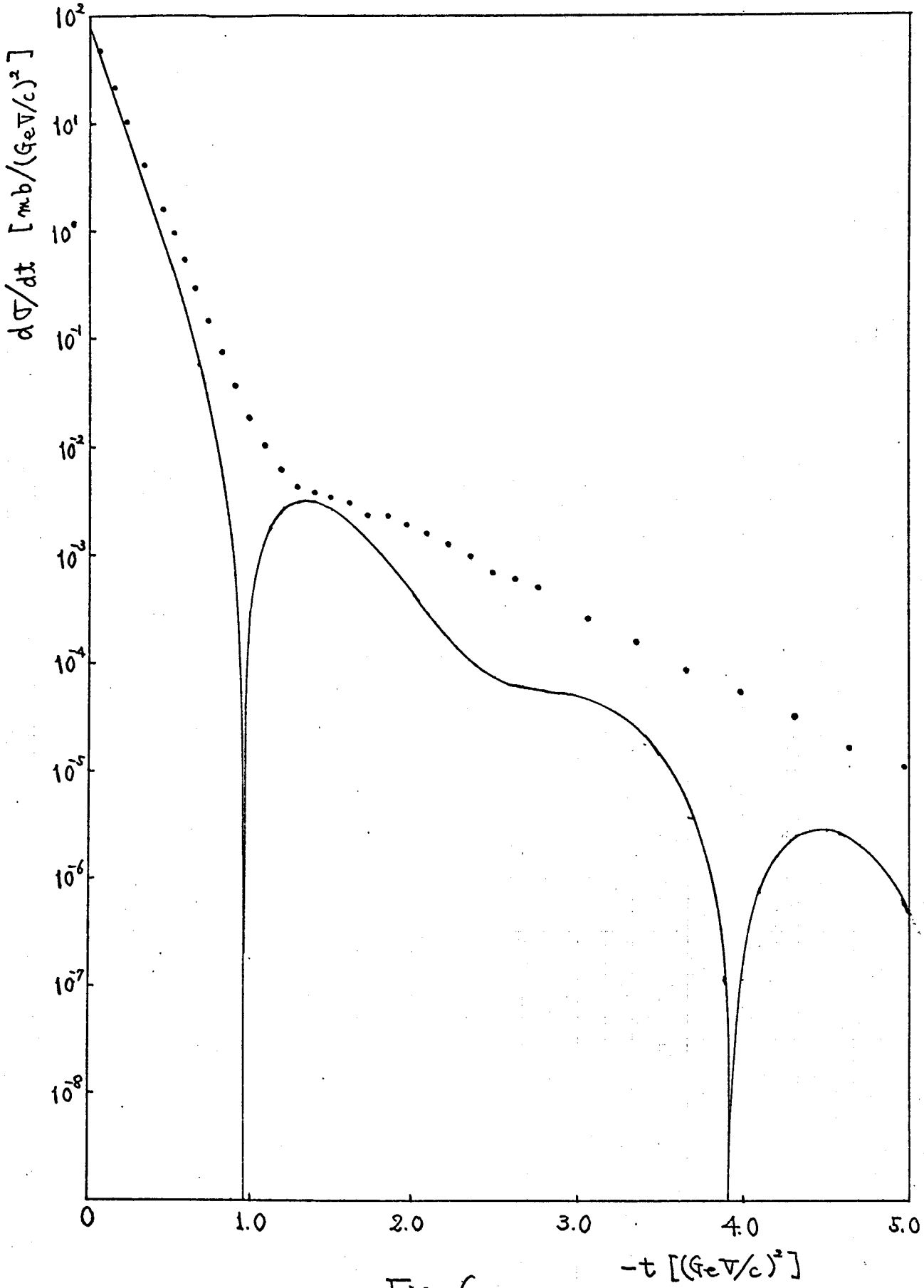
dσ/dt [mb/(GeV/c)²]
10²
10¹
10⁰
10⁻¹
10⁻²
10⁻³
10⁻⁴
10⁻⁵
10⁻⁶
10⁻⁷
10⁻⁸
0
1.0
2.0
3.0
4.0
5.0
-t [(GeV/c)²]

Fig. 6

Table. 1

n	0	1	2	3	4	5	6
σ_n [mb]	8.05	18.45	7.09	3.22	1.42	0.58	0.21
$n_{(ch)}$	0	2	4	6	8	10	12
$\sigma_{n(ch)}$ [mb]	8.7 $\pm$0.5	16.3 $\pm$8.4	11.5 $\pm$6.0	4.3 $\pm$2.5	1.9 $\pm$1.3	0.5 $\pm$0.5	0.5 $\pm$0.5